2013-12-01

PC61 (anti-CD25) treatment inhibits influenza A virus-expanded regulatory T cells and severe lung pathology during a subsequent heterologous lymphocytic choriomeningitis virus infection

Anke R.M. Kraft
University of Massachusetts Medical School

Et al.

Let us know how access to this document benefits you.

Repository Citation

Kraft AR, Wlodarczyk MF, Kenney LL, Selin LK. (2013). PC61 (anti-CD25) treatment inhibits influenza A virus-expanded regulatory T cells and severe lung pathology during a subsequent heterologous lymphocytic choriomeningitis virus infection. Morningside Graduate School of Biomedical Sciences Student Publications. https://doi.org/10.1128/JVI.00936-13. Retrieved from https://escholarship.umassmed.edu/gsbs_sp/2041

PC61 (Anti-CD25) Treatment Inhibits Influenza A Virus-Expanded Regulatory T Cells and Severe Lung Pathology during a Subsequent Heterologous Lymphocytic Choriomeningitis Virus Infection

Anke R. M. Kraft,[a,b]* Myriam F. Wlodarczyk,[a,c] Laurie L. Kenney,[a] Liisa K. Selin[a]

Department of Pathology, University of Massachusetts Medical School, Worcester, Massachusetts, USA[a]; Institute for Virology, University Hospital Essen, University of Duisburg-Essen, Essen, Germany[b]; Centre de Physiopathologie de Toulouse-Purpan INSERM UMR1043, CNRS UMR5282, Université Toulouse III CHU Purpan, Toulouse, France[c]

Prior immunity to influenza A virus (IAV) in mice changes the outcome to a subsequent lymphocytic choriomeningitis virus (LCMV) infection and can result in severe lung pathology, similar to that observed in patients that died of the 1918 H1N1 pandemic. This pathology is induced by IAV-specific memory CD8^{+} T cells cross-reactive with LCMV. Here, we discovered that IAV-immune mice have enhanced CD4^{+} Foxp3^{+} T-regulatory (Treg) cells in their lungs, leading us to question whether a modulation in the normal balance of Treg and effector T-cell responses also contributes to enhancing lung pathology upon LCMV infection of IAV-immune mice. Treg cell and interleukin-10 (IL-10) levels remained elevated in the lungs and mediastinal lymph nodes (mLNs) throughout the acute LCMV response of IAV-immune mice. PC61 treatment, used to decrease Treg cell levels, did not change LCMV titers but resulted in a surprising decrease in lung pathology upon LCMV infection in IAV-immune but not in naive mice. Associated with this decrease in pathology was a retention of Treg in the mLN and an unexpected partial clonal exhaustion of LCMV-specific CD8^{+} T-cell responses only in IAV-immune mice. PC61 treatment did not affect cross-reactive memory CD8^{+} T-cell proliferation. These results suggest that in the absence of IAV-expanded Treg cells and in the presence of cross-reactive memory, the LCMV-specific response was overstimulated and became partially exhausted, resulting in a decreased effector response. These studies suggest that Treg cells generated during past infections can influence the characteristics of effector T-cell responses and immunopathology during subsequent heterologous infections. Thus, in humans with complex infection histories, PC61 treatment may lead to unexpected results.

During a lifetime the immune system is shaped by a history of infections. Prior infections with one pathogen may influence the severity of disease outcome to a subsequent infection with an unrelated pathogen, a phenomenon known as heterologous immunity (1). Enhanced immunopathology, which can be mediated by the activation of cross-reactive memory T cells, is one of the harmful consequences of heterologous immunity. For instance, it has been proposed during human infections that cross-reactive IAV-specific memory CD8^{+} T cells can contribute to the induction of severe fulminant hepatitis during hepatitis C virus (HCV) infection and induction of acute infectious mononucleosis during Epstein-Barr virus (EBV) infection (2–4).

Lung pathology is a common manifestation of respiratory infections and can vary greatly in severity in different individuals infected with the same pathogen. To investigate the role of altered immunopathology during heterologous immunity in a controlled experimental setting, we utilized a mouse model of IAV-immune mice infected with lymphocytic choriomeningitis virus (LCMV) (5). We initially chose these two viruses because they are phylogenetically unrelated and because they are naturally spread through infection of the respiratory mucosa and induce significant inflammation in the lung (6–11). Influenza virus is an extremely common respiratory pathogen in humans, and LCMV, which induces a flu-like illness in humans, is also a relatively common pathogen, with 5 to 14% of the general population being serologically positive (12). These IAV-immune mice infected with LCMV could develop acute lung injury similar to that seen in individuals that died during the H1N1 IAV pandemic in 1918, with enhanced bronchus-associated lymphoid tissue (BALT), mononuclear pneumonia, necrotizing bronchiolitis, vasculitis, and bronchiol-

ization (13, 14) The severity of lung pathology varied among genetically identical mice from mild pneumonitis to severe mononuclear pneumonia, necrotizing bronchiolitis, and bronchiolization, an abnormal alveolar epithelial repair process considered premalignant and associated with idiopathic pulmonary fibrosis in humans. Although counterintuitive, severity of pathology did not directly correlate with LCMV titers. Instead, increased pathology was dependent on cross-reactive IAV-specific memory CD8^{+} T cells (15). Disease severity was directly correlated with and could be predicted by the frequency of two IAV epitope-specific CD8^{+} T-cell populations, PB1$_{703}$ and PA$_{224}$, which are cross-reactive with LCMV-GP$_{34}$ and -GP$_{276}$, respectively. Eradication or functional ablation of these pathogenic populations of IAV-specific memory T cells using mutant viral strains, peptide-based tolerization strategies, or short-term anti-gamma interferon (IFN-γ) treatment prevented this pathology.

Here, we continue to investigate this mouse model to determine if there are other contributing factors responsible for this variation in lung pathology and to define potential therapies. At major mucosal interfaces such as the lung, which is frequently
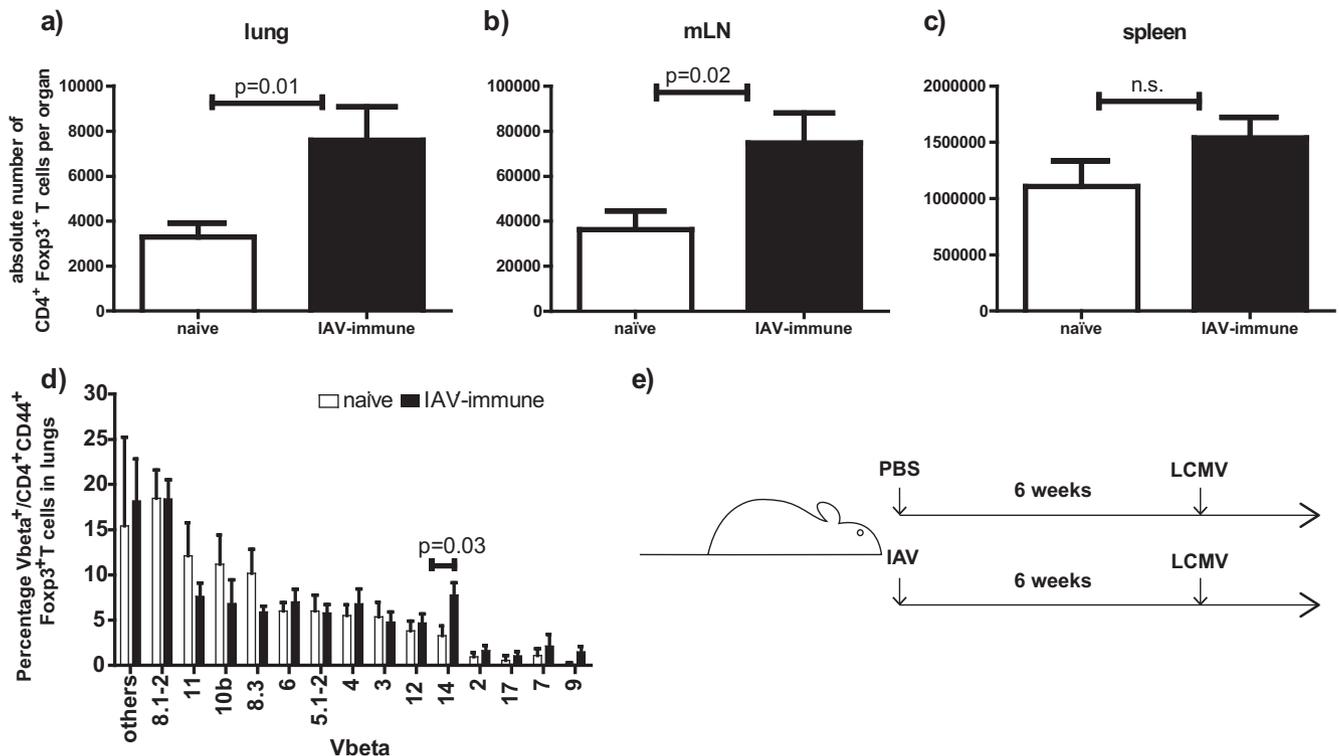
FIG 1 (a to c) Increased absolute number of regulatory CD4$^+$ Foxp3$^+$ T cells in lungs and mLNs of IAV-immune mice. Mice were infected i.n. with IAV or PBS was inoculated into controls (naive). Six weeks after infection, mice were considered immune and CD4$^+$ Foxp3$^+$ Treg cell numbers were determined by flow cytometry in lungs (a), mLNs (b), and spleens (c). Results were pooled from 2 to 3 independent experiments. Statistical analysis was done using an unpaired *t* test with 8 to 12 mice/group. (d) Treg cells in lungs of IAV-immune mice showed changes in Vβ usage consistent with IAV inducing expansion of an antigen-specific Treg cell population. Lymphocytes were isolated from lungs of IAV-immune or naive mice, and the Vβ repertoire for Treg cells was determined by MAb staining. Data shown are gated on CD4$^+$ CD44$^+$ FoxP3$^+$ T cells. Results are means ± standard errors of the means (SEM) pooled from 2 independent experiments (naïve, *n* = 7; IAV-immune, *n* = 9). (e) Experimental setup of sequential IAV and LCMV infections. Mice were infected i.n. with IAV 6 weeks prior to LCMV infection. As controls, age-matched mice were treated with PBS 6 weeks prior to LCMV infection.

exposed to foreign antigens, discrimination between innocuous and foreign antigen-specific immune responses is necessary to limit chronic inflammation. T-regulatory (Treg) cells have been shown to be key mediators in balancing inflammation and in inhibiting immune-mediated tissue damage, especially in organs like the lung and gastrointestinal tract (16–18). Both natural and induced Treg cells can suppress the function of many types of immune cells, including CD8$^+$ and CD4$^+$ T cells, B cells, dendritic cells (DC), NK cells, and NKT cells either by direct contact or by production of inhibitory cytokines, such as interleukin-10 (IL-10) and transforming growth factor beta (TGF-β) (19, 20). Treg cells have been intensively studied in autoimmunity, tumors, and persistent infections (19, 21–24). Increased numbers of Treg cells and a loss of functional virus-specific effector T cells are reported in persistent virus infections, such as hepatitis C virus (HCV), human immunodeficiency virus (HIV), Friend virus (FV), and herpes simplex virus (HSV), but not in acute virus infection (19, 25–28). Depletion of the suppressive Treg cells during a persistent retroviral infection resulted in enhanced effector T-cell function and reduced viral load (28, 29). Treg cells can also prevent extensive immunopathology during viral infections (24, 30, 31). Depletion of natural Treg cell responses, using PC61 treatment (anti-CD25) prior to infection, enhanced antiviral responses without any evidence of enhanced immunopathology if HSV-1 was injected into the footpad (32). However, Treg cell depletion prior to

corneal HSV-1 infection resulted in severe T-cell-mediated tissue lesions (33). These results suggest that Treg cells influence disease outcome during viral infection differently depending on the virus and on the site of infection. Interestingly, compared to naive age-matched mice, we observed enhanced numbers of CD4$^+$ Foxp3$^+$ Treg cells in the lungs, spleens, and draining lymph nodes of mice immune to the nonpersistent virus IAV. Therefore, we were interested in determining whether Treg cells that expanded following a viral infection could also play a role during heterologous immunity, modifying immunopathology during a subsequent unrelated infection.

MATERIALS AND METHODS

Viruses and infections of mice. Six-week-old C57BL/6 (H-2b) male mice were obtained from The Jackson Laboratory (Bar Harbor, ME). The mice were anesthetized by inhalation of metofane (Pitman-Moore, Mundelein, IL) and infected intranasally (i.n.) with 70 PFU of the mouse-adapted IAV A/PR/8/34 (H1N1) or were inoculated with phosphate-buffered saline (PBS) as a control. This virus was prepared from eggs and was not exposed to bovine serum (5). After the immune system had returned to homeostasis (6 weeks or longer), immune and control mice were challenged i.n. with 1 × 10^5 PFU of LCMV clone 13 (Fig. 1e).

In experiments examining activation of cross-reactive memory CD8$^+$ T cells, mice were infected intraperitoneally (i.p.) with 5 × 10^4 PFU of LCMV Armstrong or were inoculated with PBS as a control. After the immune system had returned to homeostasis, LCMV-immune and con-

trol mice were challenged i.p. with 2×10^7 PFU Pichinde virus (PV; AN3739 strain) (see Fig. 6a). LCMV and PV were propagated in BHK21 baby hamster kidney cells. The LCMV stock was diluted 1:100 in serum-free media, and the stocks of PV were purified through a sucrose gradient and diluted in Hanks' balanced salt solution (34). Immune mice were sex and age matched to control mice and housed under exactly the same pathogen-free conditions for the same time period. All experiments were done in compliance with institutional guidelines as approved by the Institutional Animal Care and Use Committee at the University of Massachusetts Medical School.

Virus titration. A 10% homogenate of lung and spleen tissue from each individual mouse was serially diluted and titrated on Vero cells to quantify LCMV PFU (5). Titers were reported as the arithmetic $\log_{10}$ PFU for whole lungs and spleens that had been individually titrated from four to five mice per group.

Lung histological evaluation. At days 7, 9, and 12 post-LCMV challenge, lungs from naive, IAV-immune, and Treg cell-depleted IAV-immune mice were collected, fixed in 10% neutral buffered formaldehyde, and embedded in paraffin. Tissue sections (5 μm) were stained with hematoxylin and eosin (H&E) and analyzed microscopically. Scoring of lung pathology by a pathologist blinded to the experimental design was graded based on a scale described in previously published studies (5, 15): 1, mild interstitial mononuclear infiltrates, disorganized BALT, and perivascular edema; 2, moderate interstitial mononuclear infiltrates, small amount of organized BALT, and pulmonary edema; 3, moderate interstitial mononuclear infiltrates, pulmonary edema, enhanced organized BALT, mild bronchiolization, and mild consolidation; 4, severe interstitial mononuclear infiltrates, greatly enhanced pulmonary edema, enhanced organized BALT, moderate bronchiolization, moderate consolidation, and moderate necrotizing bronchiolitis; 5, severe interstitial mononuclear infiltrates, greatly enhanced pulmonary edema, enhanced organized BALT, severe bronchiolization, severe consolidation, severe necrotizing bronchiolitis, and vasculitis involving more than half of the lung. The scoring on each individual mouse was done on 4 to 5 different sections of the lung, representing 4 to 5 different lobes of the whole lung assessing both qualitative and quantitative changes in histology. The histology photographs showing high-power 10× views of a small portion of one lobe of the lung demonstrate examples of the types of pathology observed in different treatment groups, but evaluations of the whole lung were used for scoring.

Cell surface and tetramer staining. Single-cell suspensions were prepared from spleens, mediastinal lymph nodes (mLNs), and lungs, and erythrocytes were lysed with 0.84% NH$_4$Cl solution. Splenocytes were stained as described previously (35) using CD8α (53-6.7), CD4 (GK1.5), CD44 (IM7), PD-1 (J43), and Vβ-specific monoclonal antibody (MAb). All surface antibodies were purchased from BD Biosciences (San Jose, CA). For tetramer staining, cells were incubated for 60 min with allophycocyanin (APC) or phycoerythrin (PE)-labeled tetramers. After 40 min of tetramer incubation, surface antibodies were added for 20 min. Cells were fixed in Cytofixation (BD Biosciences). Data were acquired on an LSRII fluorescence-activated cell sorter (FACS) (BD Biosciences) and were analyzed with the software FlowJo (Tree Star, Ashland, OR).

Synthetic peptides. Synthetic LCMV peptides D^b NP$_{396-404}$ (FQPQNGQFI), D^b GP$_{33-41}$ (KAVYNFATC), D^b GP$_{276-286}$ (SGVENPG GYCL), and K^b NP$_{205-212}$ (YTVKYPNL), as well as PV peptides D^b NP$_{38-45}$ (SALDFHKV) and K^b NP$_{205-212}$ (YTVKFPNM), were used in this study. Synthetic peptides were provided by Biosource International (Camarillo, CA) or 21st Century Biochemicals (Marlboro, MA) and used at a 90% level of purity.

Intracellular cytokine and Foxp3 staining. LCMV peptide-specific, IFN-γ/tumor necrosis factor alpha (TNF-α)-secreting CD8$^+$ T cells were detected using the Cytofix/Cytoperm kit plus (with GolgiPlug; BD Biosciences) as described previously (36). Splenocytes were prepared as described above. In brief, cells were incubated with 1 to 5 μM synthetic peptide and 10 U/ml of human recombinant IL-2 (BD Biosciences) for 5

h at 37°C. After surface staining, cells were permeabilized with Cytofix/Cytoperm and stained intracellularly with cytokine antibodies to IFN-γ (XMG1.2) and TNF (MP6-XT22), all purchased from BD Biosciences.

Foxp3 staining of *ex vivo*-isolated cells was performed using the Foxp3 staining kit (eBiosciences, San Diego, CA). After surface staining, cells were fixed and intracellularly stained with Foxp3 antibodies according to the manufacturer's guidelines.

Cytokine multiplex assay. Cells isolated from the spleen, lung, and mLN harvested on days 0, 1, 3, 7, 9, and 12 after LCMV infection were lysed and sent to Pierce/Searchlight (Rockford, IL) for enzyme-linked immunosorbent assay (ELISA) multiplex analysis of IL-10.

PC61 treatment to remove Treg cell activity *in vivo*. Three days prior to LCMV infection, IAV-immune mice received a single dose of 100 μg of PC61 (anti-CD25) i.p. by following a well-established protocol for removal of Treg cell activity *in vivo* (16, 33, 37, 38) (see Fig. 3a). Control mice were treated with PBS or the isotype control (rat IgG1). The same depletion protocol was used to remove Treg cell activity from naive and LCMV-immune mice prior PV infection (see Fig. 6a). These antibodies were purchased from BioExpress Inc. (Kaysville, UT). Three days post-PC61 treatment, a 95 to 98% reduction of CD25$^+$ CD4$^+$ T cells was observed in spleens, lungs, and mLNs.

Statistical analysis. Two-tailed Student's t tests were performed to compare two groups. Paired t tests were used for comparing mean values from different organs at different time points in two different treatment groups. Two-way analysis of variance (ANOVA) with Bonferroni posttest was used to compare more than two groups. Linear regression was used to measure correlation between two independent variables. Fisher's exact test was used to measure differences between categorical data, such as changes in immunodominant epitope. Statistical analysis was performed using GraphPad Prism software (San Diego, CA) (*, $P \leq 0.05$; **, $P < 0.01$; ***, $P < 0.001$).

RESULTS

Enhanced levels of Treg cells in IAV-immune mice. Compared to naive controls, a significant 2-fold increase in absolute number (Fig. 1a) and percentage (naïve mice, $0.68 \pm 0.04\%$; IAV-immune mice, $1.06 \pm 0.11\%$; $P = 0.03$; $n = 12$) of CD4$^+$ Foxp3$^+$ Treg cells was detected in the lungs of IAV-immune mice 6 weeks after i.n. infection with an associated alteration in the T-cell receptor repertoire (Fig. 1d). There was also a 2-fold increase in absolute Treg cell numbers in the draining mLNs (Fig. 1b), with no difference in the nondraining inguinal lymph nodes (iLNs) (naïve, $7.56 \times 10^4 \pm 3.4 \times 10^4$; IAV immune, $11 \times 10^4 \pm 5.2 \times 10^4$; $P = 0.6$; $n = 4$) and a small increase in the spleens (Fig. 1c). In contrast, infection with another nonpersistent virus, LCMV (Armstrong strain), did not enhance absolute number (naïve, $3.51 \times 10^4 \pm 1 \times 10^4$; LCMV-immune, $2.31 \times 10^4 \pm 1.2 \times 10^4$; $P = 0.6$; $n = 4$ to 11) or percentage (naïve, $0.68 \pm 0.04\%$; LCMV-immune, $0.82 \pm 0.11\%$; $n = 4$ to 12) of Treg cells in the lungs of LCMV-immune mice. These results suggest that some nonpersistent but potentially cytopathic viruses that induce lung pathology, such as IAV (5, 13, 14), could significantly enhance the number of Treg cells, while other viruses which induce minimal lung pathology, such as LCMV, do not. Interestingly, these increased levels of Treg cells were still detectable long after the acute IAV infection during the memory phase in the lung, the site of the virus infection, and in the draining mLN.

IAV-expanded increase in Treg cells persisted during a subsequent heterologous virus infection with LCMV. After finding increased Treg cells in the lungs and mLNs of IAV-immune mice, we questioned whether these expanded Treg cells participate in dysregulating normal immune responses, leading to either the increased lung pathology or viral titers that had been observed in IAV-immune mice acutely infected with LCMV (5, 15). First, we
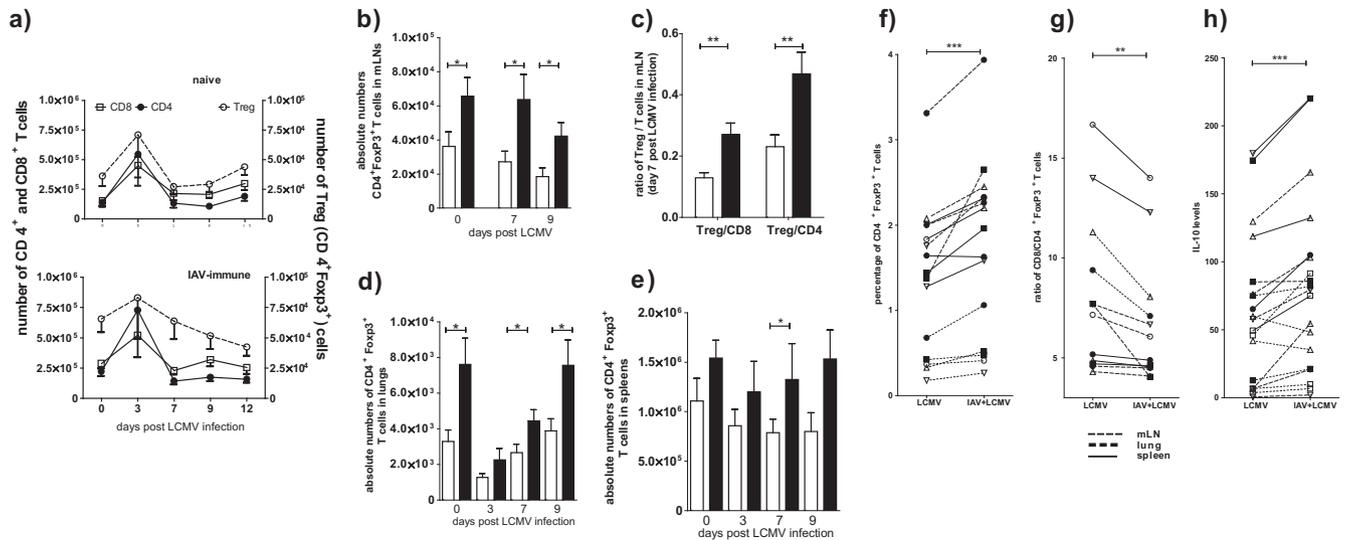
FIG 2 Increased numbers of Treg cells in mLN, lung, and spleen of IAV-immune mice during subsequent acute LCMV infection. Naive and IAV-immune mice were infected i.n. with LCMV (Fig. 1e). (a) Kinetics of CD4$^+$, CD8$^+$, or Treg cell responses after LCMV infection in naive (top) or IAV-immune mice (bottom). At the indicated time points after LCMV infection, absolute numbers of CD8$^+$, CD4$^+$, and Treg cells were determined in mLNs. (b to e) The total number of Treg cells was determined between naive (white) and IAV-immune (black) mice at the indicated time points post-LCMV infection in mLNs (b), lungs (d), and spleens (e). (c) Ratio of CD8$^+$ T cells to CD4$^+$ Foxp3$^+$ Treg cells and CD4$^+$ T cells to CD4$^+$ Foxp3$^+$ Treg cells are shown at day 7 in the mLNs. Data shown in panels a to e are pooled from 2 to 3 independent experiments with $n = 7$ to 12 mice/time point/group. Statistical analysis was done using an unpaired t test. (f and g) Overall increase in Treg cells throughout LCMV infection in IAV-immune mice. At the indicated time points, from day 0 to 12 post-LCMV infection, the percentage of Treg cells (f) and ratio of CD8$^+$ T cells to CD4$^+$ Foxp3$^+$ Treg cells (g) were determined in mLNs, lungs, and spleens. Data shown in panels f and g are pooled from 2 independent experiments with $n = 7$ to 12 mice/time point/group. This is the same data as that shown in panels a to e but analyzed using a paired Student's t test. (h) Increased IL-10 levels in IAV-immune mice during LCMV infection. Spleen, mLN, and lung cell lysates from day 0 to 12 postinfection with LCMV in naive or IAV-immune mice were analyzed with an ELISA multiplex technique for IL-10 cytokine production. Organ lysates were generated from a pool of 3 mice for each time point. Black circle, day 0; open square, day 1; open triangle, point up, day 3; black square, day 7; open triangle, point down, day 9. Each time point shows a pool of 2 independent experiments. Paired Student's t test was used to analyze data shown in panels f to h.

determined if this increased number of Treg cells in IAV-immune mice persisted throughout the subsequent LCMV infection (Fig. 1e and 2). In naive mice, all T-cell subpopulations demonstrated a similar pattern of expansion in the mLNs during acute LCMV infection, with significant 4- and 3-fold increases in total numbers of CD4$^+$ ($P = 0.002$; $n = 7$) and CD8$^+$ ($P = 0.05$; $n = 7$) T cells, respectively, by day 3. There also was a 2-fold increase in Treg cells ($P = 0.06$; $n = 7$) (Fig. 2a). By day 7, all three T-cell subpopulations had returned to preinfection levels (day 0). However, in IAV-immune mice challenged 6 weeks later with LCMV, Treg cells expanded and contracted in a manner discordant with CD4$^+$ and CD8$^+$ T cells (Fig. 2a, lower). Unexpectedly, the total number of Treg cells remained elevated from day 0 to 9 post-LCMV infection in the mLNs of IAV-immune mice (Fig. 2a and b). In fact, a significant, 2-fold higher number of Treg cells was observed on days 7 and 9 after LCMV infection in IAV-immune compared to naive mice (Fig. 2b). At day 7 post-LCMV infection, there was a significant 2-fold increase in the Treg cell/CD4$^+$Foxp3$^-$ T cell and Treg cell/CD8$^+$ T cell ratios in IAV-immune mice compared to naive mice (Fig. 2c). Since the effect of Treg cells on effector T cells is dependent upon their levels compared to each other, these data suggest that the increased number of Treg cells is able to attenuate the activation of LCMV-specific T-cell responses during their priming in the mLN.

Similar to the mLN, the absolute number of Treg cells in the lung was increased in IAV-immune mice throughout LCMV infection compared to the controls, with significant increases at days 7 and 9 (Fig. 2d). Even in the spleen the absolute number of Treg

cells was increased before and during LCMV infection, reaching a significant increase by day 9, the peak of the LCMV CD8$^+$ T-cell response, in IAV-immune mice (Fig. 2e). By using paired t tests for time point and organ (thereby eliminating the variability in cell number that occurs with time after infection and organ), we found that there was a significant overall increase of both the percentage (Fig. 2f) and total number (data not shown) of Treg cells in the lung, mLN, and spleen throughout the LCMV infection from day 0 to 12 of the IAV-immune mouse. This resulted in a decreased ratio of effector cells to Treg cells, both CD8$^+$ (Fig. 2g) and CD4$^+$ (data not shown), during the LCMV infection in IAV-immune mice compared to those of controls throughout the infection in all three organs.

As Treg cells are capable of producing inhibitory cytokines, such as IL-10, we questioned whether there was any evidence of enhanced IL-10 levels during LCMV infection in IAV-immune mice. ELISA multiplex analysis of splenic, mLN, and lung cell lysates demonstrated that IAV-immune mice had significantly higher levels of IL-10 expression than naive mice throughout the LCMV infection (Fig. 2h). Thus, it is possible that the presence of IAV-expanded Treg cells in IAV-immune mice will suppress normal immune effector responses and either decrease LCMV clearance or alter immunopathology.

PC61 treatment (anti-CD25) led to decreased lung pathology during acute LCMV infection of IAV-immune mice. In order to determine if the increased levels of Treg cells played a role in mediating immunopathology or altering viral clearance during LCMV infection of IAV-immune mice, PC61 treatment (anti-
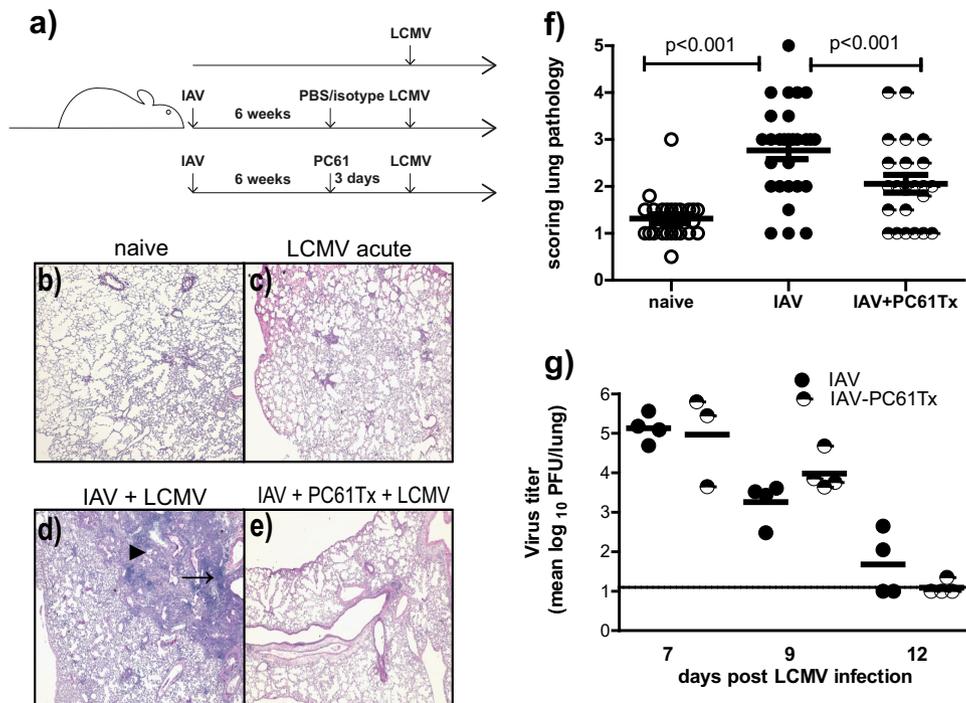
FIG 3 PC61 (anti-CD25) treatment in IAV-immune mice prior to LCMV infection resulted in significantly decreased lung pathology. (a) Experimental setup of sequential IAV and LCMV infections with PC61 treatment. Three days prior to LCMV infection, IAV-immune mice were treated i.p. with PBS/isotype or PC61 (anti-CD25) (IAV and PC61) and compared to PBS/isotype-treated naive mice. Lung pathology was analyzed at days 7 and 9 post-LCMV infection, and LCMV viral titers were determined at days 7 to 12 postinfection. (b to e) Lung histology of representative mice: naive untreated, uninfected lung (b); LCMV-infected naive with mild interstitial infiltrates (c); LCMV-infected IAV-immune mice (IAV + LCMV) with consolidation, enhanced BALT (small arrow), and bronchiolization (large arrow) (d); and Treg-depleted LCMV-infected IAV-immune mice with mild interstitial infiltrates (IAV + PC61Tx + LCMV) (e). (f) Scored lung pathology in naive, IAV-immune, and PC61-treated IAV-immune mice post-LCMV infection (pooled data from days 7 and 9 from 4 independent experiments). (g) LCMV viral titers in lungs at days 7, 9, and 12 post-LCMV infection in LCMV-infected IAV-immune and PC61-treated IAV-immune mice (representative experiment of two similar experiments). Open circle, LCMV-infected naive mice; closed, black circle, LCMV-infected IAV-immune mice; half-filled circle, LCMV-infected, PC61-treated IAV-immune mice. Statistical analysis was done using a two-way ANOVA.

CD25), a well-established conventional technique, was used to remove Treg cell activity (Fig. 3a) (16, 32, 33, 37, 38). LCMV infection i.n. in naive mice induced mild interstitial mononuclear infiltrates (Fig. 3c), whereas in IAV-immune mice it induced enhanced bronchus-associated lymphoid tissue (BALT), mononuclear pneumonic consolidations, perivascular and pulmonary edema, bronchiolitis, and bronchiolization (Fig. 3d) (5, 15). Since the presence of Treg cells is frequently associated with decreasing immunopathology, we were somewhat surprised to observe a significant reduction in the severity of lung pathology on days 7 and 9 post-LCMV infection in IAV-immune mice receiving PC61 treatment prior to challenge (Fig. 3e and f). The lung histology in many of the PC61-treated mice resembled that in naive mice infected with LCMV (Fig. 3c), with only mild mononuclear infiltrates. The vast majority of the mice scored below level 3, when bronchiolization, the pathognomonic finding of severe pathology, is first observed. There was no significant difference in weight loss (data not shown) or LCMV titers in the lungs post-LCMV challenge of PC61-treated and nontreated IAV-immune mice, suggesting that the presence of enhanced levels of Treg cells in IAV-immune mice was not altering LCMV clearance (Fig. 3g).

PC61 (anti-CD25) treatment resulted in decreased LCMV-specific CD8$^+$ T-cell responses in the spleen and lung of LCMV-infected IAV-immune mice. PC61 treatment prior to LCMV infection in IAV-immune mice led to a significant decrease in the

overall total number of LCMV-specific CD8$^+$ T cells (NP396- and GP33-specific response) in the spleen (Fig. 4a), associated with lower numbers in the lung, at days 7 and 9 postinfection compared to nontreated mice. In complete contrast, PC61 treatment resulted in a significant enhancement of the total number of LCMV-specific CD8$^+$ T cells in the draining mLN on day 7 in IAV-immune mice during LCMV challenge (Fig. 4a). In the nontreated mice, by days 7 and 9 of LCMV infection effector CD8$^+$ T cells were decreased in the mLN and might have already trafficked to the lung and spleen, sites of infection (Fig. 4a). Interestingly, there was no effect of PC61 treatment on the number of LCMV GP61-specific CD4$^+$ T cells at days 7 and 9 of LCMV infection in the spleen and mLN in IAV-immune mice (Fig. 4b).

These results suggest that there is a delay in effector CD8$^+$ T-cell trafficking out of the lymph node in the absence of Treg cells from the LCMV-infected IAV-immune mice, which is consistent with previous reports (39). This delay in effector CD8$^+$ T-cell trafficking to the spleen and lung after PC61 treatment may play some role in decreasing lung pathology.

PC61 treatment during acute LCMV infection in naive mice showed no differences in immunopathology and viral titer but did decrease LCMV-specific CD8$^+$ T-cell responses. In order to determine if the above-described findings are a phenomenon related to IAV-expanded Treg cells in the lungs and mLN following sequential infection of IAV-immune mice with LCMV or just an
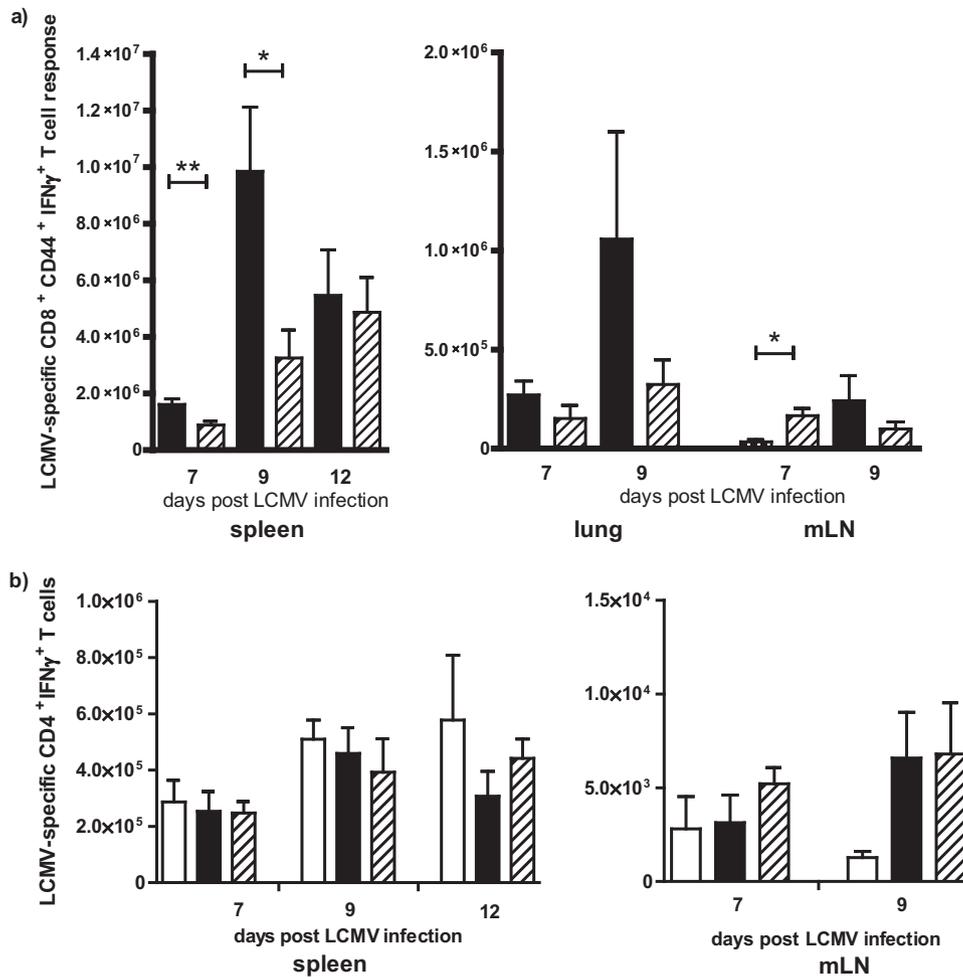
FIG 4 PC61 (anti-CD25) treatment in IAV-immune mice prior to LCMV infection resulted in decreased LCMV-specific CD8$^+$ T-cell response in the spleen and enhanced response in the mLN with no effect on the CD4$^+$ T-cell response. (a) Total number of LCMV-specific CD8$^+$ T-cell responses (NP396 + GP33) was determined in spleens, lungs, and mLNs at days 7 to 12 post-LCMV infection in PC61-treated or nontreated IAV-immune mice (the experimental setup was the same as that described in the legend to Fig. 3a). Black bar, nontreated IAV-immune mice; diagonal striped bar, PC61-treated mice. (b) Total number of LCMV GP61-specific CD4$^+$ T-cell responses were determined in spleens and mLNs from LCMV-infected nontreated naive (white bar) and nontreated (black bar) or PC61-treated (diagonally striped bar) IAV-immune mice. Data shown are from 1 to 3 pooled experiments ($n = 5$ to 15 mice/group). Statistical analysis was done using Student's t test (a) and two-way ANOVA (b).

effect of PC61 (anti-CD25) treatment prior to LCMV infection, naive mice were treated with PC61 prior to LCMV infection (Fig. 5a). Unlike the IAV-immune mice, PC61-treated naive mice had lung pathology and virus titers similar to those of control treated mice at days 5, 7, and 9 post-LCMV infection (Fig. 5b and c). However, similar to the results for IAV-immune mice (Fig. 4), PC61-treated naive mice had decreased LCMV-specific CD8$^+$ T-cell responses in the spleen and lung at days 7 and 9 post-LCMV infection compared to control-treated mice (Fig. 5d). They also had increased LCMV-specific CD8$^+$ T cells in the mLN at day 9. However, while PC61 treatment led to retention of Treg cells in the mLN, it had no effect on pathology or virus titers during acute LCMV infection of naive mice. This suggests that PC61 treatment in IAV-immune mice where Treg cells are elevated affects CD8$^+$ T cell responses during LCMV infection differently than in naive mice.

PC61 treatment during PV infection in LCMV-immune mice did not alter activation of cross-reactive NP205-specific CD8$^+$ memory T cells. PC61 treatment prior to virus infection in naive mice usually results in increasing the activation and frequency of virus-specific CD8$^+$ T cells (16, 25, 32, 38). However, it is possible that anti-CD25 treatment interferes with the activation of the cross-reactive IAV-specific memory CD8$^+$ T cells responsible for the lung pathology upon LCMV infection. In order to test this hypothesis, we utilized a heterologous virus infection model, LCMV-immune mice infected with PV, where there is no con-founding variable, such as immunopathology, and there is a strong activation of cross-reactive NP205-specific memory CD8$^+$ T cells which become immunodominant during the second virus infection (40, 41) (Fig. 6a). PC61 treatment of LCMV-immune mice prior to PV infection resulted in equally effective reactivation of the cross-reactive LCMV-NP205 memory CD8$^+$ T cells, which instead of being very subdominant during PV infection became codominant with the PV-NP38 response (Fig. 6b). Also, the NP205-specific T-cell response became immunodominant in the LCMV-specific memory response (Fig. 6c), as we have previously reported (40). These results suggest that PC61 treatment does not
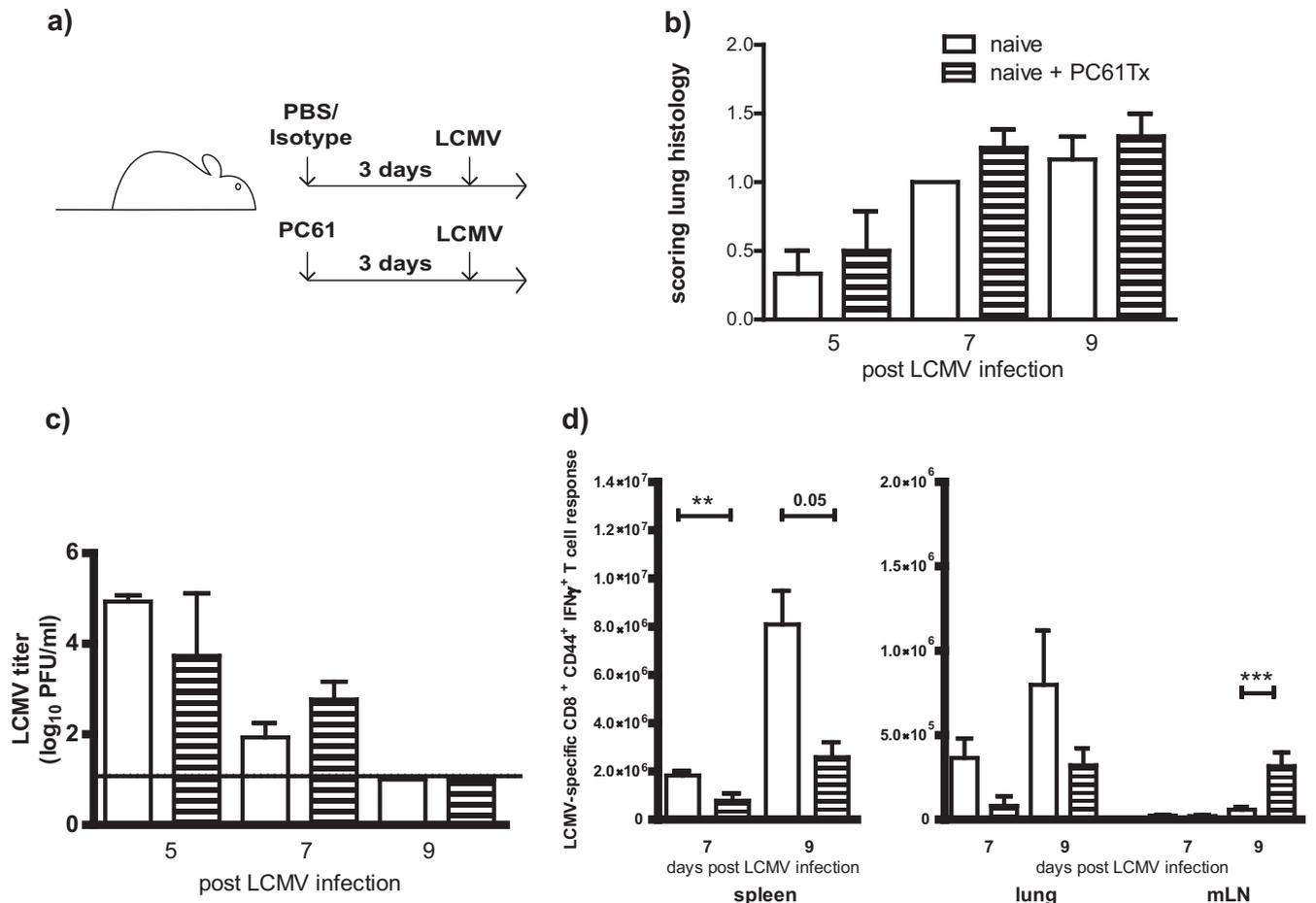
FIG 5 PC61 treatment (anti-CD25) in naive mice prior to LCMV infection had no effect on lung pathology and viral clearance. (a) Experimental setup of acute LCMV infection with PC61 treatment. To deplete Treg cells in naive mice prior to LCMV infection, PC61 treatment (anti-CD25) was injected i.p. 3 days prior to LCMV infection. As a control, naive age-matched mice were treated with PBS or the isotype control prior to LCMV infection. Lung pathology scoring (b) and viral titers (c) from LCMV-infected naive and PC61-treated naive mice at days 5, 7, and 9 post-LCMV infection are shown. (d) Total number of LCMV-specific $CD8^+$ T-cell responses (NP396 + GP33) was determined in spleens, lungs, and mLNs at days 7 and 9 post-LCMV infection in PC61-treated or nontreated mice. Naive nontreated (white bar) and PC61-treated (horizontal striped bar) mice post-LCMV infection are shown. Data shown are from 1 to 3 pooled experiments with $n = 5$ to 15 mice/group. Statistical analysis was done using Student's t test.

interfere with reactivation of cross-reactive memory cells, which is consistent with data suggesting that CD25 does not play a major role in activation of memory $CD8^+$ T cells (42).

Partial exhaustion of LCMV-specific $CD8^+$ T-cell responses might contribute to decreasing lung pathology in PC61-treated IAV-immune mice. To further investigate why PC61 treatment during LCMV infection of IAV immune mice resulted in decreased lung pathology, we questioned if decreased Treg cell function induced by PC61 treatment had any effect on the functional efficiency of the LCMV-specific $CD8^+$ T-cell responses. Loss of effector $CD8^+$ T-cell function, called exhaustion, has been described for different persistent viruses (43–45). Exhaustion of $CD8^+$ T cells can be divided into different stages with a gradual loss of T-cell functions in the following order: IL-2 production and proliferation, TNF production and cytotoxicity, and IFN-γ production (45). Partial exhaustion can occur during early periods of chronic infection or in chronic infections when the antigen load is not exceptionally high. Partially exhausted $CD8^+$ T cells are characterized by loss of TNF-α production and reduced proliferation potential (45). Additionally, upregulation of PD-1 and

changes in the immunodominance hierarchy of the antigen-specific $CD8^+$ T-cell responses can be found, as some epitope-specific responses are more sensitive to exhaustion (45–49). For instance, NP396-specific $CD8^+$ T-cell responses during chronic LCMV infection are the most sensitive to exhaustion, and this normally immunodominant response becomes subdominant or disappears completely (45). We began to question whether partial exhaustion was occurring in the IAV-immune mice treated with PC61 prior to LCMV infection, when we noticed that in the decreased LCMV-specific $CD8^+$ T-cell response (Fig. 4) there was a disproportionately greater loss of NP396-specific $CD8^+$ T cells (Fig. 7). In fact, upon closer examination, we noted that in these PC61-treated IAV-immune mice infected with LCMV, the NP396-specific TNF-α-producing $CD8^+$ T cells were significantly decreased, in contrast to the GP33-specific $CD8^+$ T cells (Fig. 7a to c). Significantly fewer NP396-specific multicytokine-producing (TNF^+ IFN-γ^+) to single cytokine-producing (TNF^- IFN-γ^+) $CD8^+$ T cells were observed in PC61-treated mice (ratio, 5.9 ± 1) compared to nontreated IAV-immune mice (2.5 ± 0.3) ($P = 0.025$; $n = 14$) (Fig. 7a). This was also associated with a decrease in the
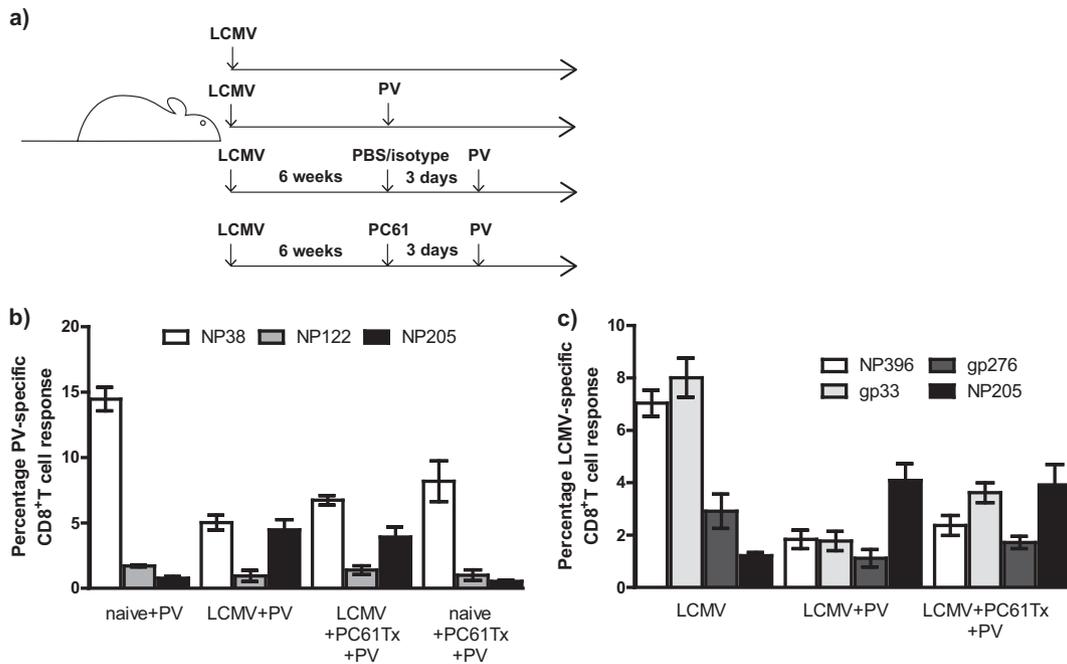
FIG 6 PC61 treatment (anti-CD25) in LCMV-immune mice prior to PV infection does not affect reactivation and immunodomination by cross-reactive NP205-specific memory CD8+ T cells. (a) Experimental setup of sequential LCMV and PV (LCMV+PV) infections with PC61 treatment. Three days prior to PV infection, LCMV-immune (LCMV) mice were treated with PBS/isotype or PC61 (anti-CD25) (LCMV+PC61) and compared to PBS/isotype-treated naive mice. LCMV and PV epitope-specific responses were determined using peptide stimulation in an intracellular cytokine assay at day 8 post-PV infection. (b) Percentage of PV-specific CD8+ T-cell responses (NP38, NP205, and NP122) was determined in spleens at day 8 post-PV infection in PC61-treated or nontreated LCMV-immune mice. (c) Percentage of LCMV-specific CD8+ T-cell responses (NP396, GP33, GP276, or NP205) was determined in spleens at day 8 post-PV infection in PC61-treated or nontreated LCMV-immune mice.

mean fluorescence intensity (MFI) of NP396-specific CD8+ T-cells, making both TNF and IFN-γ levels consistent with decreased cytokine production per cell (Fig. 7a and b).

LCMV-specific CD8+ T-cell responses have a highly predictable hierarchy during acute LCMV infection in naive mice which is not altered in IAV-immune mice (Fig. 7d). During acute LCMV infection, either NP396 or GP33/34 CD8+ T-cell responses may be more dominant, or they can be fully codominant (50). During the phases of T-cell exhaustion, the LCMV NP396-specific CD8+ T-cell response becomes nonfunctional before the GP33/34 response (45). Thus, changes in immunodominance hierarchy during LCMV infection are one way to assess the severity of clonal exhaustion. Thus, as the NP396-specific CD8+ T-cell response was becoming less functional during LCMV infection in PC61-treated IAV-immune mice, the GP33/34-specific CD8+ T-cell response became dominant more often than the NP396-specific response (Fig. 7d). This change in immunodominance hierarchy was unique to PC61-treated IAV-immune mice, as there was no significant difference in hierarchy in PC61-treated naive mice infected with LCMV (Fig. 7e).

Also consistent with ongoing partial CD8+ T-cell exhaustion, significantly enhanced PD-1 expression was observed on NP396-specific CD8+ T cells at days 7 and 9 of LCMV infection in PC61-treated IAV-immune mice compared to nontreated naive or IAV-immune mice (Fig. 7f). This difference in PD-1 expression had disappeared by day 12, when virus had cleared from these mice.

These changes in the characteristics of the LCMV-specific CD8+ T-cell responses (Fig. 7a to f), including alteration in immunodominance hierarchy (Fig. 7d), decreased TNF production

(Fig. 7a to c), and enhanced PD-1 expression (Fig. 7f), was not observed in PC61-treated naive mice infected with LCMV. Thus, Treg cell depletion using PC61 treatment did not lead to any evidence of partial clonal exhaustion upon LCMV infection in naive mice (Fig. 7e). Only when the increased numbers of Treg cells present in IAV-immune mice were depleted by PC61-treatment did the LCMV-specific CD8+ T cells demonstrate these features of partial clonal exhaustion. This decreased CD8+ T-cell response would result in decreased IFN-γ production, one of the mediators of severe lung pathology (15). These results suggest that the increased levels of IAV-expanded Treg cells is attenuating LCMV-specific CD8+ T-cell activation and preventing partial T-cell exhaustion in the presence of the higher viral loads in IAV-immune mice (5).

In the absence of functional Treg cells, the ratio of LCMV-GP33/34 to NP396 response directly correlated with the severity of lung pathology. In IAV-immune mice infected with LCMV, the severity of the lung pathology directly correlated with and was predicted by the frequency of IAV-PB1$_{703}$- and IAV-PA224-specific memory responses, which cross-reacted with LCMV-GP33/34 and -GP276, respectively (15). Eradication or functional ablation of these pathogenic memory T-cell populations, using mutant virus strains, peptide-based tolerization strategies, or short-term anti-IFN-γ treatment, inhibited severe lesions, such as bronchiolization, from occurring. In PC61-treated IAV-immune mice, the ratio of GP33/34 to NP396 CD8+ T-cell responses directly correlated with the severity of the residual lung pathology, which suggests that the greater the cross-reactive GP33/34-specific and the lower the non-cross-reactive NP396-specific CD8+
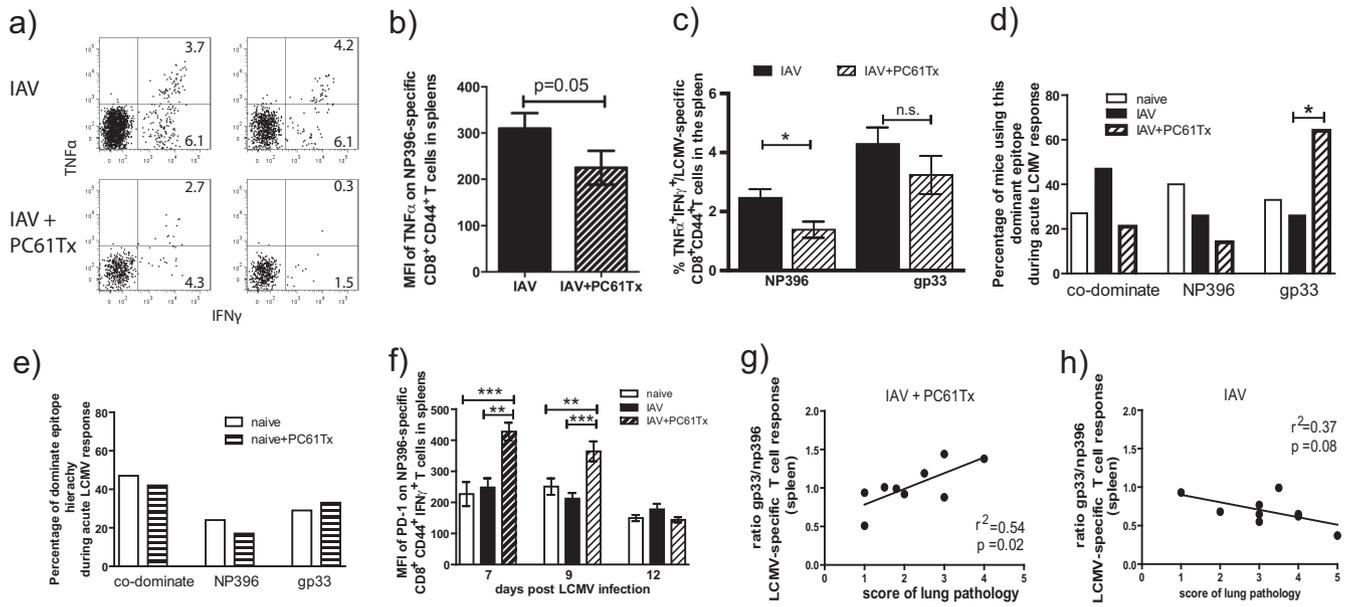
FIG 7 Partial exhaustion of LCMV-specific CD8$^+$ T-cell response may contribute to decreasing lung pathology in PC61-treated IAV-immune mice. LCMV-specific CD8$^+$ T-cell responses were determined in naive, IAV-immune, and PC61-treated IAV-immune mice post-LCMV infection (see the experimental set up described in the legend to Fig. 3a). (a to c) IFN-γ and TNF production was measured using an intracellular cytokine assay in response to LCMV-NP396 or GP33 stimulation (gated on CD8$^+$ CD44$^+$ T cells) in the spleen of nontreated (IAV) and PC61-treated IAV-immune (IAV+PC61Tx) mice at day 7 post-LCMV infection. The partial exhaustion phenotype is demonstrated by FACS plots of two representative mice showing the NP396-specific CD8$^+$ T-cell response (a), by graphing the MFI of the TNF-α^+ IFN-γ^+ NP396-specific CD8$^+$ T cell response (b), and by the percentage of TNF-α^+ IFN-γ-producing cells in either group (c). (d and e) The dominant epitope hierarchies of LCMV-specific CD8$^+$ T-cell responses in spleens at day 7 post-LCMV infection are shown from naive (white bars), IAV-immune (black bars), and PC61-treated IAV-immune mice (diagonally striped bars) (the experimental set-up is described in the legend to Fig. 3a) (d) and LCMV-infected naive (white bars) and PC61-treated naive (horizontally striped bars) mice (n = 14 to 19 mice/group from panels b and c) (the experimental set-up is described in the legend to Fig. 5a) (e). Statistical analysis used the chi-square test. (f) MFI of PD-1 on LCMV NP396-specific CD8$^+$ CD44$^+$ IFN-γ^+ T cells of LCMV-infected naive, IAV-immune, and PC61-treated IAV-immune mice at days 7, 9, and 12 post-LCMV infections in the spleen. (For this, data from Fig. 1 to 2 for pooled independent experiments with 5 to 10 mice/group and time point were used; Student's t test was used for statistical analysis). (g and h) Direct correlation of severity of lung pathology and the ratio of LCMV-specific GP33/NP396 responses in the spleen of day 9 LCMV-infected, PC61-treated IAV-immune mice (g) and day 9 LCMV-infected control nontreated IAV-immune mice (h).

T-cell response, the greater the lung pathology (Fig. 7g). This correlation was not observed in control nontreated IAV-immune mice at day 9 post-LCMV infection (Fig. 7 h). These data suggest that the partial exhaustion of the NP396-specific CD8$^+$ T-cell response in PC61-treated IAV-immune mice during LCMV challenge resulted in a greater dependence on the cross-reactive GP33/34-specific response to induce the residual pathology. This is an interesting observation, as the LCMV-GP34 CD8$^+$ T-cell response is cross-reactive with the IAV-PB1 response, and we have shown that the expansion of memory IAV-PB1-specific CD8$^+$ T cells during LCMV infection directly correlated with the severity of lung pathology (15). However, it would appear that only when we deplete the confounding influence of the Treg cells in IAV-immune mice can we observe a direct correlation between cross-reactive LCMV epitope-specific responses and severity of lung pathology. This is another indication that PC61 treatment did not affect the activation and proliferation of cross-reactive memory cells.

DISCUSSION

Recently, antigen-specific IAV-induced Treg cells have been reported to attenuate subsequent T cell responses and decrease pathology during a secondary challenge with heterosubtypic IAV infection (51, 52). Here, we show for the first time that virus-expanded Treg cells could attenuate immune responses and influ-

ence induction of lung pathology during a subsequent unrelated nonpersistent virus infection. The presence of increased Treg cells during persistent viral infections in naive mice is well documented and is known to influence viral clearance and immunopathology (19, 25–28). Our results suggest that Treg cells generated during an acute infection that clears but where tissue damage occurs can influence the qualitative characteristics of effector T-cell responses and their ability to contribute to lung pathology during a subsequent heterologous virus infection. Thus, an individual's history of infection and specific sequence of infection can alter Treg cell populations, resulting in greatly altered disease outcome during subsequent new infections.

Whereas Treg cell inactivation with PC61 treatment prior to an acute LCMV infection had no influence on the LCMV-induced immunopathology in the lung, depletion prior to LCMV infection in IAV-immune mice resulted in significantly decreased immunopathology. Increased numbers of Treg cells in IAV-immune mice appeared to attenuate activation of both non-cross-reactive and cross-reactive LCMV-specific CD8$^+$ T cells, and their presence was detrimental for the host in terms of immunopathology. In the absence of Treg cells there was a delay in effector CD8$^+$ T cells trafficking to the lung and spleen, and the non-cross-reactive NP396 CD8$^+$ T-cell response was so strongly activated that it became partially clonally exhausted, leading to decreased immunopathology. Furthermore, depletion of Treg cells in these sequen-

tially infected mice led to revealing a direct correlation between the ratio of cross-reactive LCMV GP33/34 to non-cross-reactive NP396 CD8^{+} T-cell responses and the severity of the residual lung pathology. These data suggest that prior shaping of the immune system with unrelated infections is as important as the characteristics of a specific pathogen in terms of influencing Treg cell induction and their beneficial or detrimental effects for the host.

Treg cells were increased in the lung and draining lymph node (mLN) of IAV-immune mice even 6 weeks after resolution of the acute infection. This is consistent with recent reports (51, 52) that IAV can induce IAV antigen-specific Treg cells, which can directly attenuate the function of IAV-specific effector T cell function, including proliferation and IFN-γ production. Increased Treg cells have been found in chronic virus infections like hepatitis B/C virus, HIV, and Friend virus (19, 26, 28, 53). Punkosdy et al. showed that Treg cell expansions depend on viral chronicity (54). Since replicating IAV is cleared within the first 10 days postinfection (55–57), one possibility for the significantly enhanced numbers of Treg cells in the lungs and mLNs of IAV-immune mice is the response to self-antigens presented as a result of the damaged lung tissue during acute IAV infection (5). In this case, constant self-specific antigen and T cells would still be around after IAV is cleared. This might explain why we found significantly increased Treg cell numbers in IAV-immune mice even up to several months post-IAV infection. However, it is also possible that Treg cells were maintained at significantly higher numbers due to persistent IAV-derived antigen presentation, which has been described by others (58). Jelley-Gibbs et al. showed that antigen-specific CD4^{+} T cell responses could be generated up to 3 to 4 weeks post-IAV clearance. These late primed IAV-specific CD4^{+} T cells have an intermediate phenotype with decreased contraction capacity. Interestingly, these IAV-specific CD4^{+} T cells are Vβ 4, 7, and 14 (58). Treg cells in the lungs of our IAV-immune mice showed enhanced usage of Vβ 4 and 7 and significantly enhanced Vβ 14 (Fig. 1d). This is an indication that late IAV antigen presentation has an influence on the enhanced IAV-expanded Treg cell numbers in lungs of IAV-immune mice. The results from the recently reported IAV-induced Treg studies suggest that these cells are activated in an antigen-specific manner, raising the question of whether cross-reactive LCMV-specific antigens could activate these IAV-expanded Treg cells. Our unpublished results (M. F. Wlodarczyk, A. R. M. Kraft, L. L. Kenney, E. Carter, and L. K. Selin) suggest that there are cross-reactive CD4^{+} T-cell responses between LCMV and IAV, much as we have reported cross-reactive CD8^{+} T cell responses (15).

The presence of Treg cells is usually associated with decreased immunopathology in models of autoimmune diseases, such as inflammatory bowel or celiac disease (5), and in some pathogen infections, such as respiratory syncytial virus (RSV) (16, 38) and IAV (51, 52), suggesting that depletion of Treg cells in IAV-immune mice resulted in increased lung pathology compared to nondepleted mice or even death after LCMV infection. Depletion of Treg cells by PC61 treatment prior to acute viral infection with, for instance, corneal HSV-1, neonatal HSV-1, or i.n. RSV, significantly enhances severe pathology mediated by increased virus-specific T-cell responses (16, 33, 38). These studies support the concept that the presence of Treg cells results in attenuation of effector T-cell activation. In IAV-immune mice prior to and throughout the subsequent LCMV infection, we found significantly increased numbers of IAV-expanded Treg cells and the sup-

pressive cytokine IL-10, which has been shown to decrease pathology (19, 59, 60) or contribute to induction of chronic infection with high-dose LCMV clone 13 by induction of CD8^{+} T-cell exhaustion (61–63). Thus, it was possible that depletion of Treg cell function prior to LCMV infection further increased the severity of lung pathology upon LCMV infection in IAV-immune mice. Surprisingly, depletion of Treg cells in IAV-immune mice prior to LCMV infection resulted in decreased lung pathology, with no differences in viral titers and significantly decreased LCMV-specific CD8^{+} T-cell responses in the spleen but not the mLN. These results suggest that there is a delay in effector T cells trafficking out of the lymph node in the absence of Treg cells in both the LCMV-infected IAV-immune and the naive mice, which is consistent with previous reports demonstrating that Treg cells play a role in controlling egress of effector T cells from the lymph node (39). However, Treg depletion with PC61 treatment did not alter the severity of immunopathology or viral load in naive mice infected with LCMV. In contrast to findings of Treg depletion via PC61 treatment during acute RSV or IAV infection, depletion of the IAV-expanded Treg cells during LCMV infection did not significantly enhance virus-specific T-cell responses (16, 25, 38). In stark contrast, the significant reduction in the severity of lung pathology appears to be mediated by overactivation and subsequent partial exhaustion of the LCMV-specific CD8^{+} T-cell response in LCMV-infected, Treg cell-depleted, IAV-immune mice.

High doses of LCMV clone 13 given intravenously leads to chronic infection that is thought to occur because the high antigen load drives LCMV-specific CD8^{+} T-cell exhaustion (45–48). These antigen-specific cells can be in various phases of partial to complete exhaustion thought to correlate with antigen load (45). Exhaustion includes disruption of predictable immunodominance hierarchies of the LCMV-specific CD8^{+} T-cell responses (loss of the dominant NP396-specific CD8^{+} T-cell response), impairment of functional T-cell responses, including loss of TNF-α production, and upregulation of PD-1 expression on exhausted virus-specific T cells (45). All of these parameters of exhaustion were detected on LCMV-specific CD8^{+} T cells in the spleens of Treg-depleted, IAV-immune mice but not in Treg-depleted, naive mice after LCMV infection.

Why would Treg depletion with PC61 treatment prior to LCMV infection in IAV-immune mice but not Treg depletion in naive mice result in partial exhaustion? There was no evidence to suggest that effector CD4^{+} T-cell activation and function in the IAV-immune or naive mice infected with LCMV was directly affected by the PC61 treatment. In naive mice infected with LCMV, the only effect that PC61 treatment had was to slightly decrease the size of the LCMV-specific CD8^{+} T-cell effector response in the spleen while it increased in the mLN, consistent with a delay in egress from the lymph node, a finding consistent with Treg depletion in Foxp3-DTR mice (39). A similar delay in LCMV-specific CD8^{+} effector T-cell expansion was observed in the Treg-depleted IAV-immune mice. There was no effect on the viral load or immunopathology in Treg-depleted (PC61Tx) naive mice. However, only in the IAV-immune mice did the PC61 treatment result in partial exhaustion of the non-cross-reactive NP396-specific CD8^{+} T-cell response and decreased immunopathology, as summarized in Table 1. The unique features of the LCMV response in IAV-immune mice are the presence of increased numbers of IAV-expanded Treg cells, increased IL-10 level, weakly activated cross-reactive IAV-specific memory CD8^{+} T cells with increased levels

TABLE 1 Factors contributing to decreased lung pathology in PC61-treated IAV-immune mice upon LCMV infection[a]

Parameter	Naive + LCMV	Naive + LCMV + PC61	IAV + LCMV	IAV + LCMV + PC61
Treg cells in lung and mLN	0	0	+	0
CD8 T cells in mLNs (day 7)	+	++	+	++
CD8 T cells in lung and spleen (day 7)	++	+	++	+
Lung pathology	+	+	++++	++
Virus titer	+	+	++	++
Partial exhaustion of LCMV-specific CD8 T-cell response	No	No	No	Yes
Expansion of cross-reactive CD8 memory T-cell response	NA	NA	+	+

[a] This table summarizes and compares the findings in both naive and IAV-immune mice, either treated with PC61 (+ PC61) or left untreated, prior to LCMV infection (+ LCMV). It suggests that a combination of factors, such as decreased effector cells and increased viral load in the lung and spleen at the peak of the CD8$^+$ T-cell response in IAV-immune mice, leads to partial exhaustion of LCMV-specific CD8$^+$ T-cell responses. All of these factors together would lead to decreased IFN-γ production in the lung, which is known to mediate this pathology (15) and may contribute to decreasing lung pathology in PC61-treated IAV-immune mice. NA, not applicable. + to ++++, relative level from low to high.

of IFN-γ (15), and greater viral load than that in naive mice (5) (Table 1). This contrasts with sequential infection with Pichinde virus in LCMV-immune mice, where no evidence for LCMV-expanded Treg cells existed (Fig. 1) and where a strong cross-reactive memory CD8$^+$ T-cell response rapidly expands and clears PV after infection with no significant immunopathology (40). PC61 treatment in these LCMV-immune mice did not affect activation and immunodomination of the cross-reactive NP205-specific CD8$^+$ T-cell response upon PV infection (Fig. 6), suggesting that PC61 treatment did not affect cross-reactive memory cell activation and severity of lung pathology in IAV-immune mice infected with LCMV.

It is unlikely that the IAV-expanded Treg cells had a significant effect on the activation of the cross-reactive memory T cells but instead were able to attenuate the priming of the naive, non-cross-reactive LCMV-specific CD8$^+$ T-cell responses. Depletion of these activated IAV-expanded Treg cells in this setting would allow a strong activation of these non-cross-reactive NP396-specific CD8$^+$ T-cell responses in the presence of activated cross-reactive IAV-specific memory CD8$^+$ T cells and the increased viral load observed in IAV-immune mice (5). This overactivation could lead to partial exhaustion of the LCMV-specific responses, decreased IFN-γ production, and less pathology. This is only partial exhaustion, as the LCMV infection was ultimately cleared and a persistent LCMV infection was not established (45). Based on our studies, it is interesting to speculate about studies done using PC61 treatment (anti-CD25) to prevent rejection following human kidney transplantation or in clinical trials to treat patients with multiple sclerosis (MS) (64). It has been postulated that PC61 treatment was effective, as it led to an impairment of CD8$^+$ T cells by blocking priming or depleting activated CD8$^+$ T cells. Our findings suggest another hypothesis in these cases in which large amounts of donor organ antigen or self-antigen in MS patients is

present: PC61 treatment leads to depletion of induced Treg cells, and unwanted antigen-specific CD8$^+$ T-cell responses become exhausted.

REFERENCES

1. **Welsh RM, Che JW, Brehm MA, Selin LK.** 2010. Heterologous immunity between viruses. Immunol. Rev. **235**:244–266.
2. **Clute SC, Watkin LB, Cornberg M, Naumov YN, Sullivan JL, Luzuriaga K, Welsh RM, Selin LK.** 2005. Cross-reactive influenza virus-specific CD8+ T cells contribute to lymphoproliferation in Epstein-Barr virus-associated infectious mononucleosis. J. Clin. Investig. **115**:3602–3612.
3. **Urbani S, Amadei B, Fisicaro P, Pilli M, Missale G, Bertoletti A, Ferrari C.** 2005. Heterologous T cell immunity in severe hepatitis C virus infection. J. Exp. Med. **201**:675–680.
4. **Wedemeyer H, Mizukoshi E, Davis AR, Bennink JR, Rehermann B.** 2001. Cross-reactivity between hepatitis C virus and influenza A virus determinant-specific cytotoxic T cells. J. Virol. **75**:11392–11400.
5. **Chen HD, Fraire AE, Joris I, Welsh RM, Selin LK.** 2003. Specific history of heterologous virus infections determines anti-viral immunity and immunopathology in the lung. Am. J. Pathol. **163**:1341–1355.
6. **Jakab GJ, Astry CL, Warr GA.** 1983. Alveolitis induced by influenza virus. Am. Rev. Respir. Dis. **128**:730–739.
7. **Mackenzie CD, Taylor PM, Askonas BA.** 1989. Rapid recovery of lung histology correlates with clearance of influenza virus by specific CD8+ cytotoxic T cells. Immunology **67**:375–381.
8. **Marshall DR, Olivas E, Andreansky S, La Gruta NL, Neale GA, Gutierrez A, Wichlan DG, Wingo S, Cheng C, Doherty PC, Turner SJ.** 2005. Effector CD8+ T cells recovered from an influenza pneumonia differentiate to a state of focused gene expression. Proc. Natl. Acad. Sci. U. S. A. **102**:6074–6079.
9. **Martinez Peralta LA, Laguens M, Ponzinibbio C, Laguens RP.** 1990. Infection of guinea pigs with two strains of lymphocytic choriomeningitis virus. Medicina **50**:225–229.
10. **Small BA, Dressel SA, Lawrence CW, Drake DR, III, Stoler MH, Enelow RI, Braciale TJ.** 2001. CD8(+) T cell-mediated injury in vivo progresses in the absence of effector T cells. J. Exp. Med. **194**:1835–1846.
11. **Walker DH, Murphy FA.** 1987. Pathology and pathogenesis of arenavirus infections. Curr. Top. Microbiol. Immunol. **133**:89–113.
12. **Marrie TJ, Saron MF.** 1998. Seroprevalence of lymphocytic choriomeningitis virus in Nova Scotia. Am. J. Trop. Med. Hyg. **58**:47–49.
13. **Hoffmann E, Krauss S, Perez D, Webby R, Webster RG.** 2002. Eight-plasmid system for rapid generation of influenza virus vaccines. Vaccine **20**:3165–3170.
14. **Thomas PG, Brown SA, Keating R, Yue W, Morris MY, So J, Webby RJ, Doherty PC.** 2007. Hidden epitopes emerge in secondary influenza virus-specific CD8+ T cell responses. J. Immunol. **178**:3091–3098.
15. **Wlodarczyk MF, Kraft AR, Chen HD, Kenney LL, Selin LK.** 2013. Anti-IFN-gamma and peptide-tolerization therapies inhibit acute lung injury induced by cross-reactive influenza a-specific memory T cells. J. Immunol. **190**:2736–2746.
16. **Fulton RB, Meyerholz DK, Varga SM.** 2010. Foxp3+ CD4 regulatory T cells limit pulmonary immunopathology by modulating the CD8 T cell response during respiratory syncytial virus infection. J. Immunol. **185**:2382–2392.
17. **Izcue A, Coombes JL, Powrie F.** 2006. Regulatory T cells suppress systemic and mucosal immune activation to control intestinal inflammation. Immunol. Rev. **212**:256–271.
18. **Sakaguchi S.** 2011. Regulatory T cells: history and perspective. Methods Mol. Biol. **707**:3–17.
19. **Rouse BT, Sarangi PP, Suvas S.** 2006. Regulatory T cells in virus infections. Immunol. Rev. **212**:272–286.

20. **Suri-Payer E, Fritzsching B.** 2006. Regulatory T cells in experimental autoimmune disease. Springer Semin. Immunopathol. **28:**3–16.

21. **Belkaid Y, Tarbell K.** 2009. Regulatory T cells in the control of host-microorganism interactions. Annu. Rev. Immunol. **27:**551–589.

22. **Loser K, Beissert S.** 2012. Regulatory T cells: banned cells for decades. J. Investig. Dermatol. **132:**864–871.

23. **Mittrucker HW, Kaufmann SH.** 2004. Mini-review: regulatory T cells and infection: suppression revisited. Eur. J. Immunol. **34:**306–312.

24. **Sakaguchi S, Yamaguchi T, Nomura T, Ono M.** 2008. Regulatory T cells and immune tolerance. Cell **133:**775–787.

25. **Haeryfar SM, DiPaolo RJ, Tscharke DC, Bennink JR, Yewdell JW.** 2005. Regulatory T cells suppress CD8+ T cell responses induced by direct priming and cross-priming and moderate immunodominance disparities. J. Immunol. **174:**3344–3351.

26. **Manigold T, Racanelli V.** 2007. T cell regulation by CD4 regulatory T cells during hepatitis B and C virus infections: facts and controversies. Lancet Infect. Dis. **7:**804–813.

27. **Sempere JM, Soriano V, Benito JM.** 2007. T regulatory cells and HIV infection. AIDS Rev. **9:**54–60.

28. **Zelinskyy G, Kraft AR, Schimmer S, Arndt T, Dittmer U.** 2006. Kinetics of CD8+ effector T cell responses and induced CD4+ regulatory T cell responses during Friend retrovirus infection. Eur. J. Immunol. **36:**2658–2670.

29. **Zelinskyy G, Dietze KK, Husecken YP, Schimmer S, Nair S, Werner T, Gibbert K, Kershaw O, Gruber AD, Sparwasser T, Dittmer U.** 2009. The regulatory T cell response during acute retroviral infection is locally defined and controls the magnitude and duration of the virus-specific cytotoxic T cell response. Blood **114:**3199–3207.

30. **Kronenberg M, Rudensky A.** 2005. Regulation of immunity by self-reactive T cells. Nature **435:**598–604.

31. **Tang Q, Bluestone JA.** 2008. The Foxp3+ regulatory T cell: a jack of all trades, master of regulation. Nat. Immunol. **9:**239–244.

32. **Suvas S, Kumaraguru U, Pack CD, Lee S, Rouse BT.** 2003. CD4+CD25+ T cells regulate virus-specific primary and memory CD8+ T cell responses. J. Exp. Med. **198:**889–901.

33. **Suvas S, Azkur AK, Kim BS, Kumaraguru U, Rouse BT.** 2004. CD4+CD25+ regulatory T cells control the severity of viral immunoinflammatory lesions. J. Immunol. **172:**4123–4132.

34. **Selin LK, Nahill SR, Welsh RM.** 1994. Cross-reactivities in memory cytotoxic T lymphocyte recognition of heterologous viruses. J. Exp. Med. **179:**1933–1943.

35. **Kim S-K, Cornberg M, Wang XZ, Chen HD, Selin LK, Welsh RM.** 2005. Private specificities of CD8 T cell responses control patterns of heterologous immunity. J. Exp. Med. **201:**523–533.

36. **Varga SM, Welsh RM.** 1998. Detection of a high frequency of virus-specific CD4+ T cells during acute infection with lymphocytic choriomeningitis virus. J. Immunol. **161:**3215–3218.

37. **Betts RJ, Ho AW, Kemeny DM.** 2011. Partial depletion of natural CD4CD25 regulatory T cells with anti-CD25 antibody does not alter the course of acute influenza A virus infection. PLoS One **6:**e27849. doi:10.1371/journal.pone.0027849.

38. **Ruckwardt TJ, Bonaparte KL, Nason MC, Graham BS.** 2009. Regulatory T cells promote early influx of CD8+ T cells in the lungs of respiratory syncytial virus-infected mice and diminish immunodominance disparities. J. Virol. **83:**3019–3028.

39. **Lund JM, Hsing L, Pham TT, Rudensky AY.** 2008. Coordination of early protective immunity to viral infection by regulatory T cells. Science **320:**1220–1224.

40. **Brehm MA, Pinto AK, Daniels KA, Schneck JP, Welsh RM, Selin LK.** 2002. T cell immunodominance and maintenance of memory regulated by unexpectedly cross-reactive pathogens. Nat. Immunol. **3:**627–634.

41. **Cornberg M, Chen AT, Wilkinson LA, Brehm MA, Kim SK, Calcagno C, Ghersi D, Puzone R, Celada F, Welsh RM, Selin LK.** 2006. Narrowed TCR repertoire and viral escape as a consequence of heterologous immunity. J. Clin. Investig. **116:**1443–1456.

42. **Williams MA, Tyznik AJ, Bevan MJ.** 2006. Interleukin-2 signals during priming are required for secondary expansion of CD8+ memory T cells. Nature **441:**890–893.

43. **Day CL, Kaufmann DE, Kiepiela P, Brown JA, Moodley ES, Reddy S, Mackey EW, Miller JD, Leslie AJ, DePierres C, Mncube Z, Duraiswamy J, Zhu B, Eichbaum Q, Altfeld M, Wherry EJ, Coovadia HM, Goulder

PJ, Klenerman P, Ahmed R, Freeman GJ, Walker BD.** 2006. PD-1 expression on HIV-specific T cells is associated with T cell exhaustion and disease progression. Nature **443:**350–354.

44. **Shin H, Wherry EJ.** 2007. CD8 T cell dysfunction during chronic viral infection. Curr. Opin. Immunol. **19:**408–415.

45. **Wherry EJ, Blattman JN, Murali-Krishna K, van der Most R, Ahmed R.** 2003. Viral persistence alters CD8 T cell immunodominance and tissue distribution and results in distinct stages of functional impairment. J. Virol. **77:**4911–4927.

46. **Moskophidis D, Laine E, Zinkernagel RM.** 1993. Peripheral clonal deletion of antiviral memory CD8+ T cells. Eur. J. Immunol. **23:**3306–3311.

47. **Moskophidis D, Lechner F, Pircher H, Zinkernagel RM.** 1993. Virus persistence in acutely infected immunocompetent mice by exhaustion of antiviral cytotoxic effector T cells. Nature **362:**758–761.

48. **Welsh RM, McNally JM.** 1999. Immune deficiency, immune silencing, and clonal exhaustion of T cell responses during viral infections. Curr. Opin. Microbiol. **2:**382–387.

49. **Wherry EJ.** 2011. T cell exhaustion. Nat. Immunol. **12:**492–499.

50. **Rodriguez F, Harkins S, Slifka MK, Whitton JL.** 2002. Immunodominance in virus-induced CD8(+) T cell responses is dramatically modified by DNA immunization and is regulated by gamma interferon. J. Virol. **76:**4251–4259.

51. **Bedoya F, Cheng GS, Leibow A, Zakhary N, Weissler K, Garcia V, Aitken M, Kropf E, Garlick DS, Wherry EJ, Erikson J, Caton AJ.** 2013. Viral antigen induces differentiation of Foxp3+ natural regulatory T cells in influenza virus-infected mice. J. Immunol. **190:**6115–6125.

52. **Brincks EL, Roberts AD, Cookenham T, Sell S, Kohlmeier JE, Blackman MA, Woodland DL.** 2013. Antigen-specific memory regulatory CD4+ Foxp3+ T cells control memory responses to influenza virus infections. J. Immunol. **190:**3438–3446.

53. **Francisco LM, Salinas VH, Brown KE, Vanguri VK, Freeman GJ, Kuchroo VK, Sharpe AH.** 2009. PD-L1 regulates the development, maintenance, and function of induced regulatory T cells. J. Exp. Med. **206:**3015–3029.

54. **Punkosdy GA, Blain M, Glass DD, Lozano MM, O'Mara L, Dudley JP, Ahmed R, Shevach EM.** 2011. Regulatory T cell expansion during chronic viral infection is dependent on endogenous retroviral superantigens. Proc. Natl. Acad. Sci. U. S. A. **108:**3677–3682.

55. **Brimnes MK, Bonifaz L, Steinman RM, Moran TM.** 2003. Influenza virus-induced dendritic cell maturation is associated with the induction of strong T cell immunity to a coadministered, normally nonimmunogenic protein. J. Exp. Med. **198:**133–144.

56. **Graham MB, Braciale TJ.** 1997. Resistance to and recovery from lethal influenza virus infection in B lymphocyte-deficient mice. J. Exp. Med. **186:**2063–2068.

57. **Roman E, Miller E, Harmsen A, Wiley J, Von Andrian UH, Huston G, Swain SL.** 2002. CD4 effector T cell subsets in the response to influenza: heterogeneity, migration, and function. J. Exp. Med. **196:**957–968.

58. **Jelley-Gibbs DM, Brown DM, Dibble JP, Haynes L, Eaton SM, Swain SL.** 2005. Unexpected prolonged presentation of influenza antigens promotes CD4 T cell memory generation. J. Exp. Med. **202:**697–706.

59. **Loebbermann J, Schnoeller C, Thornton H, Durant L, Sweeney NP, Schuijs M, O'Garra A, Johansson C, Openshaw PJ.** 2012. IL-10 regulates viral lung immunopathology during acute respiratory syncytial virus infection in mice. PLoS One **7:**e32371. doi:10.1371/journal.pone.0032371.

60. **Weiss KA, Christiaansen AF, Fulton RB, Meyerholz DK, Varga SM.** 2011. Multiple CD4+ T cell subsets produce immunomodulatory IL-10 during respiratory syncytial virus infection. J. Immunol. **187:**3145–3154.

61. **Brooks DG, Trifilo MJ, Edelmann KH, Teyton L, McGavern DB, Oldstone MB.** 2006. Interleukin-10 determines viral clearance or persistence in vivo. Nat. Med. **12:**1301–1309.

62. **Ejrnaes M, Filippi CM, Martinic MM, Ling EM, Togher LM, Crotty S, von Herrath MG.** 2006. Resolution of a chronic viral infection after interleukin-10 receptor blockade. J. Exp. Med. **203:**2461–2472.

63. **Maris CH, Chappell CP, Jacob J.** 2007. Interleukin-10 plays an early role in generating virus-specific T cell anergy. BMC Immunol. **8:**8. doi:10.1186/1471-2172-8-8.

64. **Schippling DS, Martin R.** 2008. Spotlight on anti-CD25: daclizumab in MS. Int. MS J. **15:**94–98.

65. **Izcue A, Coombes JL, Powrie F.** 2009. Regulatory lymphocytes and intestinal inflammation. Annu. Rev. Immunol. **27:**313–338.